Neurobiology of Aging 37 (2016) 12–18

Contents lists available at ScienceDirect

Neurobiology of Aging

journal homepage: www.elsevier.com/locate/neuaging

Physiological fluctuations in white matter are increased in Alzheimer's disease and correlate with neuroimaging and cognitive biomarkers

Ilia Makedonov [a,b], J. Jean Chen [b,c,d], Mario Masellis [e,f], Bradley J. MacIntosh [b,d,f,*], for the Alzheimer's Disease Neuroimaging Initiative

[a] Faculty of Medicine, University of Toronto, Toronto, Ontario, Canada
[b] Heart and Stroke Foundation Canadian Partnership for Stroke Recovery, Sunnybrook Research Institute, Toronto, Ontario, Canada
[c] Rotman Research Institute, Baycrest Centre for Geriatric Care, University of Toronto, Toronto, Ontario, Canada
[d] Department of Medical Biophysics, University of Toronto, Toronto, Ontario, Canada
[e] Division of Neurology, Department of Medicine, Sunnybrook Health Sciences Centre, University of Toronto, Toronto, Ontario, Canada
[f] Brain Sciences Research Program, Sunnybrook Research Institute, Toronto, Ontario, Canada

ARTICLE INFO

Article history:
Received 15 June 2015
Received in revised form 27 August 2015
Accepted 15 September 2015
Available online 21 September 2015

Keywords:
Alzheimer's disease
Neurodegeneration
Physiological noise
Pulsatility
Resting-state functional MRI
White matter

ABSTRACT

The objective of this study was to determine whether physiological fluctuations in white matter (PFWM) on resting-state functional magnetic resonance images could be used as an index of neurodegeneration and Alzheimer's disease (AD). Using resting-state functional magnetic resonance image data from participants in the Alzheimer's Disease Neuroimaging Initiative, PFWM was compared across cohorts: cognitively healthy, mild cognitive impairment, or probable AD. Secondary regression analyses were conducted between PFWM and neuroimaging, cognitive, and cerebrospinal fluid biomarkers. There was an effect of cohort on PFWM ($t = 5.08$, degree of freedom [df] $= 424$, $p < 5.7 \times 10^{-7}$), after accounting for nuisance effects from head displacement and global signal ($t > 6.16$). From the neuroimaging data, PFWM was associated with glucose metabolism ($t = -2.93$, df $= 96$, $p = 0.004$) but not ventricular volume ($p < 0.49$) or hippocampal volume ($p > 0.44$). From the cognitive data, PFWM was associated with composite memory ($t = -3.24$, df $= 149$, $p = 0.0015$) but not executive function ($p > 0.21$). PFWM was not associated with cerebrospinal fluid biomarkers. In one final omnibus model to explain PFWM ($n = 124$), glucose metabolism ($p = 0.04$) and cohort ($p = 0.008$) remained significant, as were global and head motion root-mean-square terms, whereas memory was not ($p = 0.64$). PFWM likely reflects end-arteriole intracranial pulsatility effects that may provide additional diagnostic potential in the context of AD neurodegeneration.

1. Introduction

Alzheimer's disease (AD) is the most common neurodegenerative disorder and is characterized by progressive cognitive dysfunction that interferes with daily activities and results in significant morbidity. Mild cognitive impairment (MCI) is considered the prodromal stage of Alzheimer's dementia that can predate AD by several years (Petersen et al., 2001; Sperling et al., 2011). Although the MCI period provides a potential intervention window, there are no established treatments. Furthermore, the MCI classification is increasingly viewed as heterogeneous because not all MCI individuals convert to AD (Ganguli et al., 2011; Nettiksimmons et al., 2014).

AD-related progression is influenced by multiple pathophysiological changes, notably amyloid deposition (Lee et al., 2014; Thal et al., 2002), cerebral amyloid angiopathy (Vinters et al., 1990), and new evidence of AD pathogenesis within pericytes (Bell et al., 2012). Increasingly, cerebrovascular techniques are used to characterize small vessel disease phenomena that contribute to neurodegeneration (Honjo et al., 2012). Central and cerebral hemodynamic measures, such as arterial stiffening, carotid artery stiffening, and cerebral blood flow, are predictors of cognitive performance (Mitchell et al., 2011), cognitive decline (Scuteri et al., 2007), and AD diagnosis (Alsop et al., 2008; Johnson et al., 2005). Work by others provides support for the theory of mechanical

* Corresponding author at: Brain Sciences Research Program, Sunnybrook Research Institute, 2075 Bayview Ave., Rm M6-180, Toronto, Ontario, Canada M4N 3M5. Tel.: +416 480 6100 ×7277; fax: +416 480 4223.
E-mail address: bmac@sri.utoronto.ca (B.J. MacIntosh).

0197-4580/$ – see front matter © 2016 Elsevier Inc. All rights reserved.
http://dx.doi.org/10.1016/j.neurobiolaging.2015.09.010

factors of arterial aging (O'Rourke and Hashimoto, 2007), which leads to excessive intracranial pulsatility (described as windkessel dysfunction) in normal and demented older adult cohorts (Bateman et al., 2008; Wahlin et al., 2014).

In the present study, we use a summary measure of physiological noise in white matter (WM), which we reported on previously in a group with small vessel disease (Makedonov et al., 2013), to serve as a proxy index of cerebrovascular dysfunction, whereby elevated arterial pulsatility contributes to increased image temporal variance observed in WM on resting-state functional magnetic resonance imaging (rs-fMRI). Rs-fMRI has traditionally been used in AD to study gray matter functional connectivity, such as reported decreased co-activation of default mode network (Zhou et al., 2010). Although WM rs-fMRI signals are viewed as nuisance variables in gray matter connectivity analyses (Chai et al., 2012; Fox et al., 2009), they also provide non-neuronal physiological contrast because of cardiac pulsatility (Dagli et al., 1999; Makedonov et al., 2013; Shmueli et al., 2007), vasomotion in ischemia (Wang et al., 2008), and cerebrovascular impairment (Jahanian et al., 2014). To date, there are few rs-fMRI studies that specifically investigate WM (Ding et al., 2013; Makedonov et al., 2013); therefore, our primary objective is to compare physiological fluctuations in WM (PFWM) among normal older controls, MCI, and AD groups. We hypothesize that there will be an effect of group on PFWM from among other factors that can influence this rs-fMRI summary measure. Our secondary objective was to determine whether PFWM was associated with any established markers of AD pathology and/or neurodegeneration. For this secondary objective, neuroimaging, cognitive, and cerebrospinal fluid (CSF) data are considered. For neuroimaging markers, we used glucose metabolism, ventricular volume, and hippocampal volume. The former reflects altered bioenergetics reported in AD (Landau et al., 2011), whereas the latter 2 are structural markers of neurodegeneration and AD (Jack et al., 1992; Nestor et al., 2008). For the cognitive measures, composite scores of memory and executive function, developed from Alzheimer's Disease Neuroimaging Initiative (ADNI), were considered (Crane et al., 2012). Last, the following AD pathologic markers were also considered from CSF: amyloid-beta 1–42 peptide and tau and phosphorylated tau protein levels (Shaw et al., 2009). Secondary analyses were conducted in this manner (i.e., separately) to capture the largest subsample size for each of the association tests.

2. Methods

2.1. ADNI dataset

Data were obtained from the ADNI database (adni.loni.usc.edu). ADNI was launched in 2003 by the National Institute on Aging, the National Institute of Biomedical Imaging and Bioengineering, the Food and Drug Administration, private pharmaceutical companies, and nonprofit organizations. The primary goal of ADNI has been to test whether serial MRI, positron emission tomography, other biological markers, and clinical/neuropsychological assessment can be combined to measure the progression of MCI and early AD. ADNI is the result of efforts of many co-investigators from a broad range of academic institutions and private corporations, and participants have been recruited from >50 sites across the United States and Canada.

2.2. Ethics statement

Participants gave written informed consent at the time of enrollment and completed questionnaires approved by each participating site's institutional review board.

2.3. Participants

Only data from ADNI-2 and ADNI-GO were used because ADNI-1 did not include rs-fMRI. Participants with rs-fMRI within the first year of participation in the study were selected, which amounted to 437 rs-fMRI datasets for the primary objective. First-year data were selected to minimize potential retention bias from repeat scans. Available rs-fMRI and corresponding structural T1 images were acquired between June 30, 2010 and May 12, 2014 (downloaded in June 2014). Sample sizes for the secondary objectives were smaller because of the inclusion of rs-fMRI with other measures (i.e., matched samples with neuroimaging, cognitive, or CSF data).

2.3.1. Normal controls, MCI, and AD criteria

Participants were enrolled if they were between 55 and 90 years old, spoke English or Spanish as the first language, and completed at least 6 years of schooling. Diagnostic classification was made by ADNI investigators using established criteria (McKhann et al., 1984, 2011; Petersen et al., 1999), albeit early and late MCI groups were combined into a single MCI group. Controls had Mini-Mental Status Examination (MMSE) (Folstein et al., 1975) scores between 24 and 30 and no significant memory concerns. MCI adults had MMSE scores between 24 and 30; memory complaint; objective memory loss as quantified by the Wechsler Memory Scale Logical Memory II Test (Wechsler, 1997); a Clinical Dementia Rating (Morris, 1993) score of 0.5; lack of cognitive impairment in other domains such as executive function, visuospatial function, and language; relative sparing of activities of daily living; and absence of frank dementia. Participants in the AD cohort fulfilled the NINCDS-ADRA (National Institute of Neurological and Communicative Disorders and Stroke and the Alzheimer's Disease and Related Disorders Association) criteria for probable AD.

2.4. MRI acquisition

MR images were collected on 3-T Philips MRI systems (Philips, Amsterdam, The Netherlands) from a total of 13 sites using a standardized protocol (Jack et al., 2008). Data from 3-T MRI systems were considered (and not 1.5 T) because physiological sources in fMRI are field-strength dependent (Triantafyllou et al., 2005). T1 images were acquired with an echo time of 3 ms, a repetition time (TR) of 7 ms, flip angle of 9°, slice thickness of 1.2 mm, and a matrix size of 256 × 256 × 170. Rs-fMRI echo planar images were acquired with an echo time of 30 ms, TR of 3000 ms, flip angle of 80°, slice thickness of 3.3 mm, and a matrix size of 64 × 64 × 48 (<5% of rs-fMRI data were collected with a TR of 2250 ms).

2.5. MRI preprocessing

Preprocessing of the structural T1 images involved bias field correction using a histogram peak-sharpening algorithm (N3) (Sled et al., 1998). Echo-planar rs-fMRIs were corrected for head motion using MCFLIRT, a tool that is part of the FMRIB Software Library (Jenkinson et al., 2002). Next, the mean relative root-mean-square (RMS) head displacement (millimeter) was determined from FMRIB Software Library's MCFLIRT and used as a nuisance regressor. In addition, a global rs-fMRI signal from within-skull voxels (i.e., brain parenchyma and ventricles) was also used as a second nuisance regressor, extracted from the global signal time series. Global RMS in units of signal intensity was then calculated on the demeaned global time series. The rs-fMRI preprocessing steps were chosen based on the following rationale: 1) WM signals tend to be spatially consistent and robust in rs-fMRI (Zuo et al., 2010), hence the appeal of a PFWM summary measure; 2) the use of voxel-wise regression of motion traces may not be indicated for this

application as it may introduce spatially nonuniform effects across the WM (Satterthwaite et al., 2013); and 3) both global RMS and head displacement RMS can be viewed as confound effects that could each contribute to PFWM, of which case the latter is reported as strongly related to frame-to-frame change in signal (Power et al., 2012; Satterthwaite et al., 2013). Head displacement and global RMS regressors were included in the group-level model for all analyses (see Section 2.7).

Previously, we have shown that PFWM correlates with cardiac pulsatility in WM. We confirmed our findings by comparing conventional rs-fMRI and high temporal resolution rs-fMRI (TR of 250 ms) in young and older adults, demonstrating that aliasing of the cardiac signal in conventional fMRI data did not significantly influence this outcome (Makedonov et al., 2013). In the present study, PFWM was calculated in native rs-fMRI space using a similar method to the previous report (Makedonov et al., 2013). Step 1: isolate per voxel (i.e., x, y, z) physiological fluctuations in the rs-fMRI time series by computing the following equation:

$$PF_{x,y,z} = \sqrt{\sigma^2_{x,y,z} - \sigma^2_{thermal}}$$

Thermal noise variance ($\sigma^2_{thermal}$) was determined as the average variance in a user-defined region of interest (ROI) placed outside the brain in a corner of each resting-state image. The placement of the background ROI was chosen to minimize contribution from echo-planar imaging ghosting artifact and evaluated by histogram inspection. Step 2: the physiological noise from step 1 was normalized by the mean signal intensity in each voxel, producing a fractional blood oxygenation level–dependent change map (see examples in Fig. 1). Step 3: PFWM was calculated as the mean physiological noise across WM voxels and used as a summary metric (see subsequently on PFWM adjustment for head motion). To facilitate quality control by visual inspection, PFWM maps were registered to a common template space, by affine transformation and by using the T1 structural image as an intermediate transformation. The common template was created by randomly selecting 15 participants from each cohort (45 in total) and coregistering the T1 images to a common template using Advanced Normalization Tools. T1 images were brain extracted and segmented into CSF, gray matter, and WM tissue classes. WM masks were eroded using a 3-mm Gaussian kernel. The medulla, pons, midbrain, and cerebellum were removed from rs-fMRI to focus the analysis on WM found in the telencephalon.

2.6. Secondary analyses on biomarker measures

Ventricular volume, hippocampal volume, and fludeoxyglucose (FDG) metabolism were used as neuroimaging biomarkers. Composite scores of memory and executive function and protein levels in CSF were ascertained from the ADNI database. ADNI ventricular volumes were calculated as described by Nestor et al. (2008). Both ventricular and hippocampal volume were normalized by total

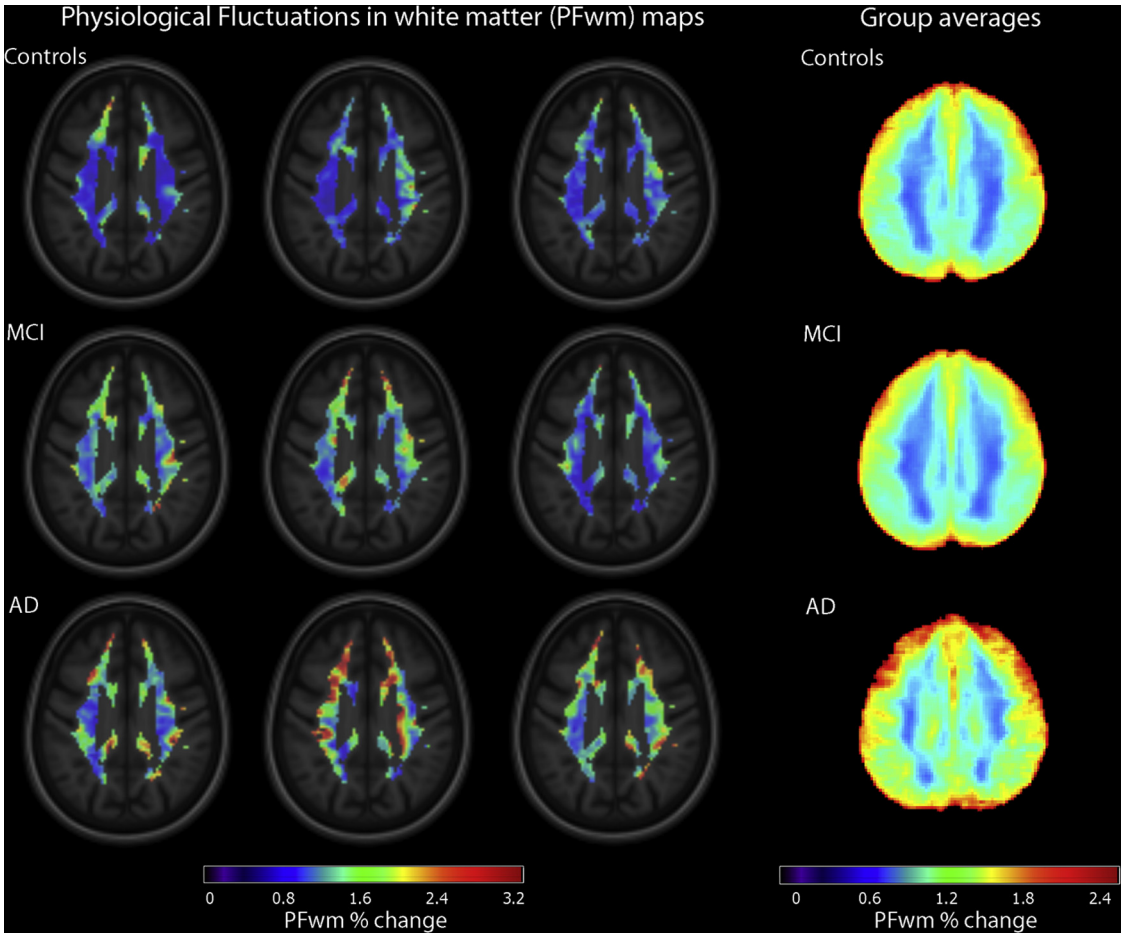

Fig. 1. Physiological fluctuations in white matter (PFWM) color maps in axial view for 3 representative participants in each cohort and overlaid on a group template T1-weighted image. Top row: controls, middle row: mild cognitive impairment (MCI), and bottom row: Alzheimer's disease (AD). The right column shows the average physiological fluctuation maps by cohort.

intracranial volume. For the FDG metabolism intensity normalized images, a composite gray matter ROI mask was used to generate a single glucose metabolism value from 5 regions identified by Landau et al. (2011) (i.e., left and right angular gyri, left and right inferior temporal gyri, and bilateral posterior cingulate cortex). Cognitive composite scores for executive function and memory were computed by Crane et al. (2012) using factor analysis. CSF protein concentrations (pictogram per milliliter) were calculated by the University of Pennsylvania ADNI Biomarker Laboratory, as described in the work of Shaw et al. (2009).

2.7. Statistics

Primary and secondary analyses were conducted using R (version 3.1.2 from RStudio, Inc). The primary analysis used a univariate linear model (analysis of variance [ANOVA], type III) and included the following independent variables: cohort, age, visit, WM volume, head displacement RMS, global RMS, and site, of which case cohort was the primary variable of interest. For secondary analyses involving subsamples, PFWM (adjusted for global and head RMS terms) was compared against ventricular volume, hippocampal volume, and glucose metabolism. Adjusted PFWM was also compared with composite measures of memory and executive function. Adjusted PFWM was compared with protein levels in CSF. The final regression test was performed using all variables that were found to correlate with PFWM, with specific interest in the effect of cohort on PFWM.

3. Results

Characteristics of the sample drawn from ADNI are summarized in Table 1. There were cohort differences that included MMSE scores ($p < 0.001$) and age (ANOVA, $p < 0.05$, controls were older on average) but no differences in gender (chi squared, $p = 0.70$), years of education ($p = 0.42$, ANOVA), or age at onset of symptoms for MCI and AD cohorts ($p = 0.79$, t test).

PFWM was significantly associated with cohort (Fig. 2, $t = 5.08$, degree of freedom [df] = 424, $p = 5.6 \times 10^{-7}$), head motion RMS ($t = 12.65$, df = 424, $p = 2 \times 10^{-7}$), and global RMS ($t = 6.16$, df = 424, $p = 1.68 \times 10^{-9}$), whereas age ($p = 0.075$) and site ($p = 0.062$) were associated with nonsignificant trends. The effects of visit ($p = 0.51$) and WM volume ($p = 0.31$) were not significant.

Table 1
Sample characteristics

	Controls	MCI	AD	*p* Value
Participants	53	102	34	
Total rs-fMRI datasets	117	246	74	
Average visits per participant	2.2	2.1	2.2	
Age at baseline (y, mean ± SD)	75.5 ± 6.7	71.9 ± 7.7	72.5 ± 7.1	<0.05
Gender (M/F)	32/21	49/53	16/18	0.70
Education (y ± SD)	16.5 ± 2.2	16.1 ± 2.6	15.8 ± 2.9	0.42
Onset of symptoms (y ± SD)	—	67.5 ± 8.1	67.1 ± 8.0	0.79
MMSE (mean of all time points ± SD)	28.9 ± 1.5	27.4 ± 2.2	21.5 ± 3.5	<0.001
Clinical Dementia Rating (median)	0	0.5	1	<0.001
FAQ (mean ± SD)	0.5 ± 2.4	3.6 ± 5.0	16.0 ± 7.1	<0.001
Cerebrospinal fluid (subsample size)	16	47	5	
Amyloid-beta level (mean ± SD)	174.8 ± 45.0	173.8 ± 58.2	126.9 ± 13.9	0.23
Tau level (mean ± SD)	71.2 ± 37.4	94.0 ± 60.1	130.4 ± 70.2	0.04
Phosphorylated tau level (mean ± SD)	33.4 ± 11.9	45.0 ± 25.2	62.0 ± 22.5	0.01

Key: AD, Alzheimer's disease; F, female; FAQ, Functional Assessment Questionnaire; M, male; MCI, mild cognitive impairment; MMSE, Mini-Mental State Examination; rs-fMRI, resting-state functional magnetic resonance image; SD, standard deviation.

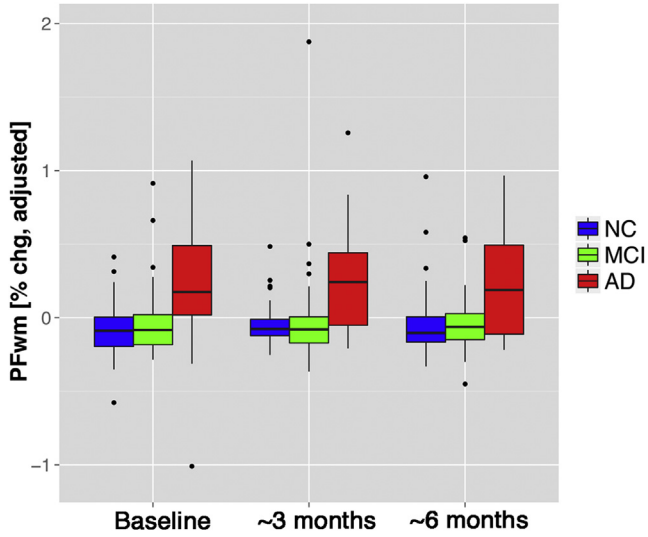

Fig. 2. Physiological fluctuations in white matter (PFWM) box plots are plotted by cohort and visit (within year 1). Controls (blue), mild cognitive impairment (MCI) (green), and Alzheimer's disease (AD) (red) are shown by different color bars. PFWM values are in units of percent blood oxygenation level–dependent (BOLD) signal change and are adjusted for head displacement and global signal root-mean-square BOLD signal (global root mean square). Visits were centered at baseline and at 3 and 6 months using k-means clustering. Cohort was a significant predictor of adjusted physiological fluctuations ($t = 5.08$, degree of freedom = 424, $p = 6 \times 10^{-7}$). (For interpretation of the references to color in this figure legend, the reader is referred to the Web version of this article.)

Adjusted PFWM was associated with regional glucose metabolism (Fig. 3A, $t = -2.93$, df = 96, $p = 0.0042$) but not ventricular volume ($p = 0.49$) nor hippocampal volume ($p = 0.44$). Note these data were extracted from samples that had all these neuroimaging measures available to permit a direct comparisons with PFWM. Adjusted PFWM was not associated with any of the CSF biomarkers ($p > 0.73$ with df = 63). For the cognitive composite scores, adjusted PFWM was correlated with composite memory (Fig. 3B, $t = -2.69$, df = 148, $p = 0.0079$) but not composite executive function ($t = -0.97$, df = 148, $p = 0.34$). In the final regression model that included cohort, glucose metabolism, composite memory, and head and global RMS variables, cohort and glucose metabolism were significant ($t = 2.71$, $p = 0.0078$ and $t = -2.07$, $p = 0.040$, respectively, for df = 117), as were head displacement RMS and global RMS ($t = 11.23$, $p = 2 \times 10^{-16}$, and $t = 6.97$, $p = 2 \times 10^{-10}$, respectively, for df = 117), whereas composite memory was not ($p = 0.63$).

4. Discussion

Rs-fMRI data from ADNI were used to investigate PFWM as a source of cerebrovascular contrast in 3 cognitive groups. We found support for our primary hypothesis: PFWM was significantly increased in AD compared with the MCI and control groups. Secondary regression analyses were conducted on subsets of ADNI participants to support the relevance of PFWM to established biomarkers. PFWM was inversely correlated with regional gray matter glucose metabolism from the neuroimaging data and inversely correlated with the memory from the cognitive composite score data. Glucose metabolism and cohort remained as significantly associated with PFWM, whereas memory was not, when each of these variables were included in one omnibus model.

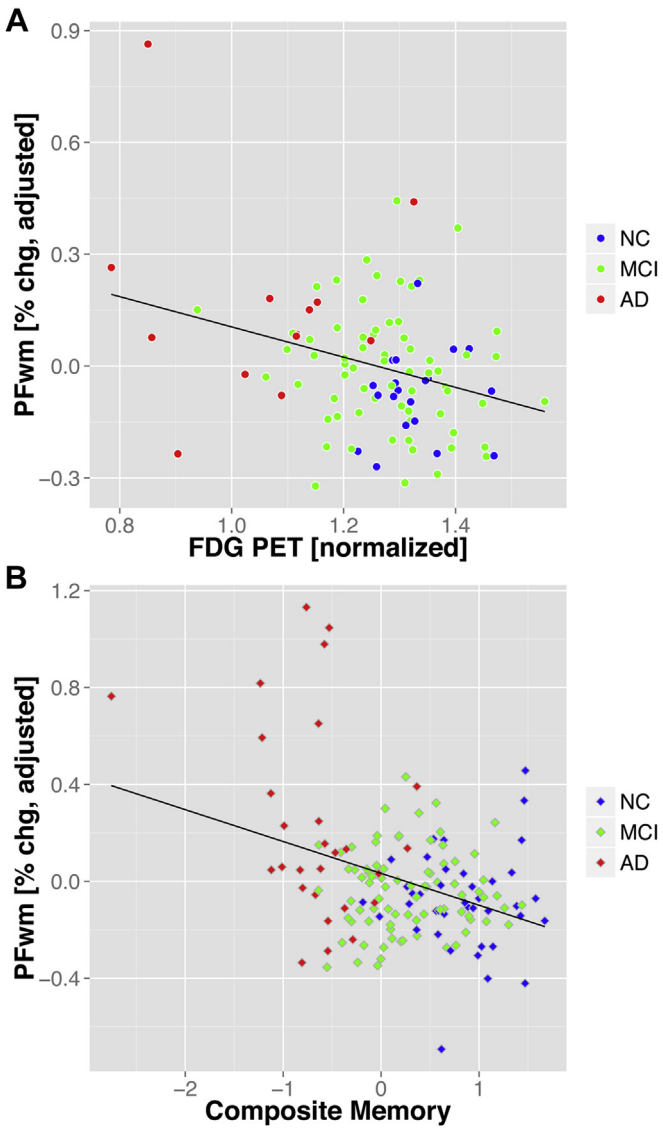

Fig. 3. Scatter plots were used to visualize regression results from single-visit data. Physiological fluctuations in white matter (PFWM) (adjusted for head displacement and global root mean square) is plotted against (A) fludeoxyglucose (FDG) metabolism ($t = -2.93$, degree of freedom = 96, $p = 0.004$, intensity normalization FDG) and (B) the composite memory score ($t = -2.69$, df = 148, $p = 0.008$). Abbreviations: AD, Alzheimer's disease; chg, change; MCI, mild cognitive impairment; NC, normal controls.

Multiple pathophysiological sources could contribute to our findings of increased PFWM in AD. Amyloid angiopathy and tortuous arterioles in WM are reported in AD, and this could explain why PFWM was increased in the current sample of AD participants (Brown et al., 2009). Mechanistically, altered cerebrovascular compliance (Thomas et al., 2014) and/or increased transmission of arterial pulsatility effects into WM could explain elevated PFWM (Dagli et al., 1999; Makedonov et al., 2013), which is consistent with the previous findings on intracranial pulsatility (Bateman et al., 2008; Wahlin et al., 2014). Although these physiological phenomena may not be purely AD etiology, mixed AD and cerebrovascular disease is recognized as the most common clinical dementia and raises questions about the role of cerebrovascular dysfunction in cognitive decline. Indeed, Scuteri et al. (2007) reported that systemic arterial stiffness was a strong predictor of cognitive decline among older adults with memory problems. Microvascular aberrations such as thickening of the basement membrane, luminal narrowing, and endothelial compression decrease vascular compliance (de la Torre, 2002), which would contribute to propagation of higher pulsatility down the vascular system and into tissue. A future direction for the present study is to consider PFWM in the context of diffusion tensor imaging; however, both diffusion tensor imaging and rs-fMRI are unfortunately not available for the same participants in ADNI. Such an analysis would speak to WM changes, such as demyelination and axonal and tissue volume changes, that occur in AD and could influence rs-fMRI WM signals (Thomas et al., 2014).

Results of our secondary analyses suggest that PFWM may have merit as a new and complimentary imaging biomarker to study neurodegeneration. Although intracranial pulsatility is reported to be associated with increased ventricular volume (Wahlin et al., 2014), we failed to detect a significant association of PFWM with ventricular or with hippocampal volume, whereas, we did find that PFWM was negatively associated with glucose metabolism in the Landau ROIs (Landau et al., 2011), which are regions that continue to be implicated in AD (Langbaum et al., 2009). Both the correlation analysis of adjusted PFWM with the biomarkers and the full-model stepwise backward regression demonstrate that adjusted PFWM provides unique information with respect to cohort. We believe that this was the case because PFWM provides physiological information that is not captured by the 4 biomarkers that were tested in this study; hence, the between-cohort differences in PFWM may reflect underlying differences in cerebrovascular health. Furthermore, brain pulsatility can be characterized by various means and has demonstrated diagnostic merit in neurodegenerative research (Bateman et al., 2008; Scuteri et al., 2007; Wahlin et al., 2014).

It is important to discuss limitations of the present study. First, we have previously shown that it is ideal to isolate cardiac pulsatility effects on rs-fMRI, particularly among adults with diffuse WM hyperintensities (WMHs) (Makedonov et al., 2013); however, this requires high temporal resolution rs-fMRI to sample the cardiac signals that was not part of the ADNI rs-fMRI. Second, despite our previous findings (Makedonov et al., 2013), we did not include WMH lesion volume in the present study. Although WMH small vessel disease has been linked to vascular pulsatility measures (Mitchell et al., 2011), at the time of this study, the ADNI sample appears to exhibit low WMH burden levels (Ramirez et al., 2015); thus, future considerations are warranted. Third, cardiac monitoring by pulse oximetry was also not part of the ADNI rs-fMRI data collection. This limits our ability to characterize PFWM in relation to heart rate during rs-fMRI. Similarly, it remains to be seen whether the respiratory cycle influences PFWM. Fourth, although the sample size for our primary objective was large, our secondary analyses were performed on subsets of participants because of the need for multiple datasets (e.g., samples with rs-fMRI and FDG-positron emission tomography). This also speaks to the challenges of considering longitudinal analysis of the ADNI data because at the time of this study, there were insufficient rs-fMRI scans beyond 1 year. It would be useful to replicate our findings from the secondary analysis as ADNI data accumulate. Furthermore, it would be useful to consider rs-fMRI data beyond 1 year in ADNI, which was an inclusion criterion by necessity because of the smaller number of samples and the need to address retention bias, specifically in the AD cohort.

In summary, this study demonstrates that physiological fluctuations can be extracted from WM regions in rs-fMRI data and used to study neurodegeneration. PFWM was robustly different between the cognitive cohorts and was associated with established neuroimaging and cognitive biomarkers of AD. PFWM may, therefore, be useful in characterizing the vascular complications associated with AD.

Disclosure statement

The authors have no conflicts of interest to disclose.

Acknowledgements

This study was funded by the Canadian Institutes of Health Research (CIHR CSE133351). Data collection and sharing for this project were funded by the Alzheimer's Disease Neuroimaging Initiative (ADNI) (National Institutes of Health Grant U01 AG024904) and DOD ADNI (Department of Defense award number W81XWH-12-2–0012). ADNI is funded by the National Institute on Aging, the National Institute of Biomedical Imaging and Bioengineering, and through generous contributions from the following: Alzheimer's Association; Alzheimer's Drug Discovery Foundation; Araclon Biotech; BioClinica, Inc; Biogen Idec Inc; Bristol-Myers Squibb Company; Eisai Inc; Elan Pharmaceuticals, Inc; Eli Lilly and Company; EuroImmun; F. Hoffmann-La Roche Ltd and its affiliated company Genentech, Inc; Fujirebio; GE Healthcare; IXICO Ltd; Janssen Alzheimer Immunotherapy Research & Development, LLC; Johnson & Johnson Pharmaceutical Research & Development, LLC; Medpace, Inc; Merck & Co, Inc; Meso Scale Diagnostics, LLC; NeuroRx Research; Neurotrack Technologies; Novartis Pharmaceuticals Corporation; Pfizer, Inc; Piramal Imaging; Servier; Synarc, Inc; and Takeda Pharmaceutical Company. The CIHR is providing funds to support ADNI clinical sites in Canada. Private sector contributions are facilitated by the Foundation for the National Institutes of Health. The grantee organization is the Northern California Institute for Research and Education, and the study is coordinated by the Alzheimer's Disease Cooperative Study at the University of California, San Diego. ADNI data were disseminated by the Laboratory for Neuro Imaging at the University of Southern California. We would also like to thank all volunteers and their families for their time and commitment. Without them, ADNI could not exist.

References

Alsop, D.C., Casement, M., de Bazelaire, C., Fong, T., Press, D.Z., 2008. Hippocampal hyperperfusion in Alzheimer's disease. Neuroimage 42, 1267–1274.

Bateman, G.A., Levi, C.R., Schofield, P., Wang, Y., Lovett, E.C., 2008. The venous manifestations of pulse wave encephalopathy: windkessel dysfunction in normal aging and senile dementia. Neuroradiology 50, 491–497.

Bell, R.D., Winkler, E.A., Singh, I., Sagare, A.P., Deane, R., Wu, Z., Holtzman, D.M., Betsholtz, C., Armulik, A., Sallstrom, J., Berk, B.C., Zlokovic, B.V., 2012. Apolipoprotein E controls cerebrovascular integrity via cyclophilin A. Nature 485, 512–516.

Brown, W.R., Moody, D.M., Thore, C.R., Anstrom, J.A., Challa, V.R., 2009. Microvascular changes in the white mater in dementia. J. Neurol. Sci. 283, 28–31.

Chai, X.J., Castanon, A.N., Ongur, D., Whitfield-Gabrieli, S., 2012. Anticorrelations in resting state networks without global signal regression. Neuroimage 59, 1420–1428.

Crane, P.K., Carle, A., Gibbons, L.E., Insel, P., Mackin, R.S., Gross, A., Jones, R.N., Mukherjee, S., Curtis, S.M., Harvey, D., Weiner, M., Mungas, D., 2012. Development and assessment of a composite score for memory in the Alzheimer's Disease Neuroimaging Initiative (ADNI). Brain Imaging Behav. 6, 502–516.

Dagli, M.S., Ingeholm, J.E., Haxby, J.V., 1999. Localization of cardiac-induced signal change in fMRI. Neuroimage 9, 407–415.

de la Torre, J.C., 2002. Alzheimer disease as a vascular disorder: nosological evidence. Stroke 33, 1152–1162.

Ding, Z., Newton, A.T., Xu, R., Anderson, A.W., Morgan, V.L., Gore, J.C., 2013. Spatio-temporal correlation tensors reveal functional structure in human brain. PLoS One 8, e82107.

Folstein, M.F., Folstein, S.E., McHugh, P.R., 1975. "Mini-mental state." A practical method for grading the cognitive state of patients for the clinician. J. Psychiatr. Res. 12, 189–198.

Fox, M.D., Zhang, D., Snyder, A.Z., Raichle, M.E., 2009. The global signal and observed anticorrelated resting state brain networks. J. Neurophysiol. 101, 3270–3283.

Ganguli, M., Snitz, B.E., Saxton, J.A., Chang, C.C., Lee, C.W., Vander Bilt, J., Hughes, T.F., Loewenstein, D.A., Unverzagt, F.W., Petersen, R.C., 2011. Outcomes of mild cognitive impairment by definition: a population study. Arch. Neurol. 68, 761–767.

Honjo, K., Black, S.E., Verhoeff, N.P., 2012. Alzheimer's disease, cerebrovascular disease, and the beta-amyloid cascade. Can. J. Neurol. 39, 712–728.

Jack Jr., C.R., Bernstein, M.A., Fox, N.C., Thompson, P., Alexander, G., Harvey, D., Borowski, B., Britson, P.J., L. Whitwell, J., Ward, C., Dale, A.M., Felmlee, J.P., Gunter, J.L., Hill, D.L., Killiany, R., Schuff, N., Fox-Bosetti, S., Lin, C., Studholme, C., DeCarli, C.S., Krueger, G., Ward, H.A., Metzger, G.J., Scott, K.T., Mallozzi, R., Blezek, D., Levy, J., Debbins, J.P., Fleisher, A.S., Albert, M., Green, R., Bartzokis, G., Glover, G., Mugler, J., Weiner, M.W., 2008. The Alzheimer's disease neuroimaging initiative (ADNI): MRI methods. J. Magn. Reson. Imaging 27, 685–691.

Jack Jr., C.R., Petersen, R.C., O'Brien, P.C., Tangalos, E.G., 1992. MR-based hippocampal volumetry in the diagnosis of Alzheimer's disease. Neurology 42, 183–188.

Jahanian, H., Ni, W.W., Christen, T., Moseley, M.E., Kurella Tamura, M., Zaharchuk, G., 2014. Spontaneous BOLD signal fluctuations in young healthy subjects and elderly patients with chronic kidney disease. PLoS One 9, e92539.

Jenkinson, M., Bannister, P., Brady, M., Smith, S., 2002. Improved optimization for the robust and accurate linear registration and motion correction of brain images. Neuroimage 17, 825–841.

Johnson, N.A., Jahng, G.H., Weiner, M.W., Miller, B.L., Chui, H.C., Jagust, W.J., Gorno-Tempini, M.L., Schuff, N., 2005. Pattern of cerebral hypoperfusion in Alzheimer disease and mild cognitive impairment measured with arterial spin-labeling MR imaging: initial experience. Radiology 234, 851–859.

Landau, S.M., Harvey, D., Madison, C.M., Koeppe, R.A., Reiman, E.M., Foster, N.L., Weiner, M.W., Jagust, W.J., 2011. Associations between cognitive, functional, and FDG-PET measures of decline in AD and MCI. Neurobiol. Aging 32, 1207–1218.

Langbaum, J.B., Chen, K., Lee, W., Reschke, C., Bandy, D., Fleisher, A.S., Alexander, G.E., Foster, N.L., Weiner, M.W., Koeppe, R.A., Jagust, W.J., Reiman, E.M., 2009. Categorical and correlational analyses of baseline fluorodeoxyglucose positron emission tomography images from the Alzheimer's Disease Neuroimaging Initiative (ADNI). Neuroimage 45, 1107–1116.

Lee, M.J., Seo, S.W., Na, D.L., Kim, C., Park, J.H., Kim, G.H., Kim, C.H., Noh, Y., Cho, H., Kim, H.J., Yoon, C.W., Ye, B.S., Chin, J., Jeon, S., Lee, J.M., Choe, Y.S., Lee, K.H., Kim, J.S., Kim, S.T., Lee, J.H., Ewers, M., Werring, D.J., Weiner, M.W., 2014. Synergistic effects of ischemia and beta-amyloid burden on cognitive decline in patients with subcortical vascular mild cognitive impairment. JAMA Psychiatry 71, 412–422.

Makedonov, I., Black, S.E., Macintosh, B.J., 2013. BOLD fMRI in the white matter as a marker of aging and small vessel disease. PLoS One 8, e67652.

McKhann, G., Drachman, D., Folstein, M., Katzman, R., Price, D., Stadlan, E.M., 1984. Clinical diagnosis of Alzheimer's disease: report of the NINCDS-ADRDA Work Group under the auspices of Department of Health and Human Services Task Force on Alzheimer's Disease. Neurology 34, 939–944.

McKhann, G.M., Knopman, D.S., Chertkow, H., Hyman, B.T., Jack Jr., C.R., Kawas, C.H., Klunk, W.E., Koroshetz, W.J., Manly, J.J., Mayeux, R., Mohs, R.C., Morris, J.C., Rossor, M.N., Scheltens, P., Carrillo, M.C., Thies, B., Weintraub, S., Phelps, C.H., 2011. The diagnosis of dementia due to Alzheimer's disease: recommendations from the National Institute on Aging-Alzheimer's Association workgroups on diagnostic guidelines for Alzheimer's disease. Alzheimers Dement. 7, 263–269.

Mitchell, G.F., van Buchem, M.A., Sigurdsson, S., Gotal, J.D., Jonsdottir, M.K., Kjartansson, O., Garcia, M., Aspelund, T., Harris, T.B., Gudnason, V., Launer, L.J., 2011. Arterial stiffness, pressure and flow pulsatility and brain structure and function: the Age, Gene/Environment Susceptibility—Reykjavik study. Brain 134 (Pt 11), 3398–3407.

Morris, J.C., 1993. The Clinical Dementia Rating (CDR): current version and scoring rules. Neurology 43, 2412–2414.

Nestor, S.M., Rupsingh, R., Borrie, M., Smith, M., Accomazzi, V., Wells, J.L., Fogarty, J., Bartha, R., Alzheimer's Disease Neuroimaging Initiative, 2008. Ventricular enlargement as a possible measure of Alzheimer's disease progression validated using the Alzheimer's disease neuroimaging initiative database. Brain 131 (Pt 9), 2443–2454.

Nettiksimmons, J., DeCarli, C., Landau, S., Beckett, L., Alzheimer's Disease Neuroimaging Initiative, 2014. Biological heterogeneity in ADNI amnestic mild cognitive impairment. Alzheimers Dement. 10, 511–521 e511.

O'Rourke, M.F., Hashimoto, J., 2007. Mechanical factors in arterial aging: a clinical perspective. J. Am Coll. Cardiol. 50, 1–13.

Petersen, R.C., Doody, R., Kurz, A., Mohs, R.C., Morris, J.C., Rabins, P.V., Ritchie, K., Rossor, M., Thal, L., Winblad, B., 2001. Current concepts in mild cognitive impairment. Arch. Neurol. 58, 1985–1992.

Petersen, R.C., Smith, G.E., Waring, S.C., Ivnik, R.J., Tangalos, E.G., Kokmen, E., 1999. Mild cognitive impairment: clinical characterization and outcome. Arch. Neurol. 56, 303–308.

Power, J.D., Barnes, K.A., Snyder, A.Z., Schlaggar, B.L., Petersen, S.E., 2012. Spurious but systematic correlations in functional connectivity MRI networks arise from subject motion. Neuroimage 59, 2142–2154.

Ramirez, J., McNeely, A.A., Scott, C.J., Masellis, M., Black, S.E., Alzheimer's Disease Neuroimaging Initiative, 2015. White matter hyperintensity burden in elderly cohort studies. The Sunnybrook Dementia Study, Alzheimer Disease Neuroimaging Initiative, and Three-City Study. Alzheimers Dement. pii: S1552-5260(15)02123-8. http://dx.doi.org/10.1016/j.jalz.2015.06.1886. [Epub ahead of print].

Satterthwaite, T.D., Elliott, M.A., Gerraty, R.T., Ruparel, K., Loughead, J., Calkins, M.E., Eickhoff, S.B., Hakonarson, H., Gur, R.C., Gur, R.E., Wolf, D.H., 2013. An improved framework for confound regression and filtering for control of motion artifact in the preprocessing of resting-state functional connectivity data. Neuroimage 64, 240–256.

Scuteri, A., Tesauro, M., Appolloni, S., Preziosi, F., Brancati, A.M., Volpe, M., 2007. Arterial stiffness as an independent predictor of longitudinal changes in cognitive function in the older individual. J. Hypertens 25, 1035–1040.

Shaw, L.M., Vanderstichele, H., Knapik-Czajka, M., Clark, C.M., Aisen, P.S., Petersen, R.C., Blennow, K., Soares, H., Simon, A., Lewczuk, P., Dean, R., Siemers, E., Potter, W., Lee, V.M., Trojanowski, J.Q., Alzheimer's Disease Neuroimaging Initiative, 2009. Cerebrospinal fluid biomarker signature in Alzheimer's disease neuroimaging initiative subjects. Ann. Neurol. 65, 403–413.

Shmueli, K., van Gelderen, P., de Zwart, J.A., Horovitz, S.G., Fukunaga, M., Jansma, J.M., Duyn, J.H., 2007. Low-frequency fluctuations in the cardiac rate as a source of variance in the resting-state fMRI BOLD signal. Neuroimage 38, 306–320.

Sled, J.G., Zijdenbos, A.P., Evans, A.C., 1998. A nonparametric method for automatic correction of intensity nonuniformity in MRI data. IEEE Trans. Med. Imaging 17, 87–97.

Sperling, R.A., Aisen, P.S., Beckett, L.A., Bennett, D.A., Craft, S., Fagan, A.M., Iwatsubo, T., Jack Jr., C.R., Kaye, J., Montine, T.J., Park, D.C., Reiman, E.M., Rowe, C.C., Siemers, E., Stern, Y., Yaffe, K., Carrillo, M.C., Thies, B., Morrison-Bogorad, M., Wagster, M.V., Phelps, C.H., 2011. Toward defining the preclinical stages of Alzheimer's disease: recommendations from the National Institute on Aging-Alzheimer's Association workgroups on diagnostic guidelines for Alzheimer's disease. Alzheimers Dement. 7, 280–292.

Thal, D.R., Rub, U., Orantes, M., Braak, H., 2002. Phases of A beta-deposition in the human brain and its relevance for the development of AD. Neurology 58, 1791–1800.

Thomas, B.P., Liu, P., Park, D.C., van Osch, M.J., Lu, H., 2014. Cerebrovascular reactivity in the brain white matter: magnitude, temporal characteristics, and age effects. J. Cereb. Blood Flow Metab. 34, 242–247.

Triantafyllou, C., Hoge, R.D., Krueger, G., Wiggins, C.J., Potthast, A., Wiggins, G.C., Wald, L.L., 2005. Comparison of physiological noise at 1.5 T, 3 T and 7 T and optimization of fMRI acquisition parameters. Neuroimage 26, 243–250.

Vinters, H.V., Secor, D.L., Pardridge, W.M., Gray, F., 1990. Immunohistochemical study of cerebral amyloid angiopathy. III. Widespread Alzheimer A4 peptide in cerebral microvessel walls colocalizes with gamma trace in patients with leukoencephalopathy. Ann. Neurol. 28, 34–42.

Wahlin, A., Ambarki, K., Birgander, R., Malm, J., Eklund, A., 2014. Intracranial pulsatility is associated with regional brain volume in elderly individuals. Neurobiol. Aging 35, 365–372.

Wang, H.H., Menezes, N.M., Zhu, M.W., Ay, H., Koroshetz, W.J., Aronen, H.J., Karonen, J.O., Liu, Y., Nuutinen, J., Wald, L.L., Sorensen, A.G., 2008. Physiological noise in MR images: an indicator of the tissue response to ischemia? J. Magn. Reson. Imaging 27, 866–871.

Wechsler, D.W., 1997. Memory Scale. Psychol. Corp, San Antonio, TX.

Zhou, J., Greicius, M.D., Gennatas, E.D., Growdon, M.E., Jang, J.Y., Rabinovici, G.D., Kramer, J.H., Weiner, M., Miller, B.L., Seeley, W.W., 2010. Divergent network connectivity changes in behavioural variant frontotemporal dementia and Alzheimer's disease. Brain 133 (Pt 5), 1352–1367.

Zuo, X.N., Kelly, C., Adelstein, J.S., Klein, D.F., Castellanos, F.X., Milham, M.P., 2010. Reliable intrinsic connectivity networks: test-retest evaluation using ICA and dual regression approach. Neuroimage 49, 2163–2177.